Germline biallelic *PIK3CG* mutations in a multifaceted immunodeficiency with immune dysregulation

Marini Thian,[1,2,3,4] Birgit Hoeger,[1,2,3] Anton Kamnev,[1] Fiona Poyer,[5] Sevgi Köstel Bal,[1,2,3] Michael Caldera,[3] Raúl Jiménez-Heredia,[1,2,3] Jakob Huemer,[1,2,3] Winfried F. Pickl,[6] Miriam Groß,[7] Stephan Ehl,[7] Carrie L. Lucas,[8] Jörg Menche,[3] Caroline Hutter,[2,5] Andishe Attarbaschi,[5] Loïc Dupré[1,9] and Kaan Boztug[1,2,3,4,5]

[1]Ludwig Boltzmann Institute for Rare and Undiagnosed Diseases, Vienna, Austria; [2]St. Anna Children's Cancer Research Institute (CCRI), Vienna, Austria; [3]CeMM Research Center for Molecular Medicine of the Austrian Academy of Sciences, Vienna, Austria; [4]Department of Pediatrics and Adolescent Medicine, Medical University of Vienna, Vienna, Austria; [5]St. Anna Children's Hospital, Department of Pediatrics and Adolescent Medicine, Medical University of Vienna, Vienna, Austria; [6]Institute of Immunology, Center for Pathophysiology, Infectiology and Immunology, Medical University of Vienna, Vienna, Austria; [7]Institute for Immunodeficiency, Center for Chronic Immunodeficiency (CCI), Medical Center - University of Freiburg, Faculty of Medicine, University of Freiburg, Freiburg, Germany; [8]Department of Immunobiology, Yale University School of Medicine, New Haven, CT, USA and [9]Center for Pathophysiology of Toulouse Purpan, INSERM UMR1043, CNRS UMR5282, Paul Sabatier University, Toulouse, France

Correspondence: KAAN BOZTUG - kaan.boztug@ccri.at

doi:10.3324/haematol.2019.231399

Supplementary Materials for

Germline biallelic *PIK3CG* mutations in a multifaceted immunodeficiency with immune dysregulation

Marini Thian[1,2,3,4], Birgit Hoeger[1,2,3], Anton Kamnev[1], Fiona Poyer[5], Sevgi Köstel Bal[1,2,3], Michael Caldera[3], Raúl Jiménez-Heredia[1,2,3], Jakob Huemer[1,2,3], Winfried F. Pickl[6], Miriam Groß[7], Stephan Ehl[7,8], Carrie L. Lucas[9], Jörg Menche[3], Caroline Hutter[2,5], Andishe Attarbaschi[5], Loïc Dupré[1,10] and Kaan Boztug[1,2,3,4,5]

[1]Ludwig Boltzmann Institute for Rare and Undiagnosed Diseases, Vienna, Austria.
[2]St. Anna Children's Cancer Research Institute (CCRI), Vienna, Austria.
[3]CeMM Research Center for Molecular Medicine of the Austrian Academy of Sciences, Vienna, Austria.
[4]Department of Pediatrics and Adolescent Medicine, Medical University of Vienna, Vienna, Austria.
[5]St. Anna Children's Hospital, Department of Pediatrics and Adolescent Medicine, Medical University of Vienna, Vienna, Austria.
[6]Institute of Immunology, Center for Pathophysiology, Infectiology and Immunology, Medical University of Vienna, Vienna, Austria.
[7]Institute for Immunodeficiency, Center for Chronic Immunodeficiency (CCI), Medical Center - University of Freiburg, Faculty of Medicine, University of Freiburg, Freiburg, Germany.
[8]Center for Pediatrics and Adolescent Medicine, Medical Center – University of Freiburg, Faculty of Medicine, University of Freiburg, Freiburg, Germany.
[9]Department of Immunobiology, Yale University School of Medicine, New Haven, CT, USA.
[10]Center for Pathophysiology of Toulouse Purpan, INSERM UMR1043, CNRS UMR5282, Paul Sabatier University, Toulouse, France.

Corresponding author:

Kaan Boztug, MD

St. Anna Children's Cancer Research Institute (CCRI) and Ludwig Boltzmann Institute for Rare and Undiagnosed Diseases

Zimmermannplatz 10, Vienna, Austria

kaan.boztug@ccri.at

MATERIALS AND METHODS

Whole Exome Sequencing and analysis

Whole exome sequencing was performed using a TruSeq Rapid Exome kit as well as the Illumina HiSeq3000/4000 system and the cBot cluster generation instruments as previously described,[1,2] with minor changes. Briefly, reads were aligned to the human genome version 19 by means of the Burrows-Wheeler Aligner (BWA). VEP was used for annotating single nucleotide variants (SNVs) and insertions/deletions lists. The obtained list was then filtered according to the presence of variants with a minor allele frequency (MAF) >0.01 in 1,000 Genomes, gnomAD, and dbSNP build 149. After further filtering steps for nonsense, missense, and splice-site variants using VCF.Filter software,[3] an internal database was used to filter for recurrent variants. Moreover, variants were prioritized using tools, such as SIFT, Polyphen-2 and the combined annotation dependent depletion (CADD) score,[4,5] that predict the deleteriousness of a present variant.

Sanger sequencing

Sanger sequencing was used to validate the two variants found in *PIK3CG*:

variant 1, ENST00000359195.3:c.145C>A, p.Arg49Ser; and variant 2, ENST00000359195.3:c.3254A>G, p.Asn1085Ser, in the affected patient and her family members. This was done by designing specific primers for the two variants.

For variant 1,

Fw1: 5’- CATGTACGCCGCCTATACCT -3’,

Rv1: 5’- TACCACTGCCCCTTCTTCTG -3’;

and for variant 2,

Fw2: 5’- TCCTGTTCTCCATGATGCTG-3’,

Rv2: 5’- AACAATCAGCAATGCCAACA-3’.

Cell Culture

Human PBMCs were isolated by Ficoll-Paque PLUS (GE Healthcare) density gradient centrifugation, washed twice in PBS, and resuspended in complete RPMI-1640 media (Gibco) containing 10 % heat-inactivated FBS, 1 % penicillin and streptomycin (Invitrogen) and 1 % HEPES buffer solution 1 M (Invitrogen). CTL and NK-cell degranulation was assessed by CD107a surface staining for 3 h in presence or absence of dynabeads human T-activator CD3/CD28 (Thermo Fisher Scientific) stimulation or K562 target cells respectively. The erythroleukemic cell line K562 (ATCC, CCL-243) was used as target cell line. NK cells were cultured in complete RPMI-1640 media with or without 600 U mL^{-1} IL-2 (Peprotech) for 48h to assess NK-cell degranulation of activated or non-activated NK cells respectively. Proliferative response was measured by labeling PBMCs with 1 mM Violet Proliferation Dye 450 (BD Biosciences) according to manufacturer's instructions. For T-cell activation and proliferation assay, PBMCs were stimulated with 2 μg mL^{-1} anti-CD3 (OKT3, Thermo Fisher Scientific) or with 1 μg mL^{-1} anti-CD28 (Thermo Fisher Scientific) or 5 μg mL^{-1} PHA (Sigma-Aldrich) for 1-3 days. PI3Kγ inhibitor IPI-549 was used at 1μM. For B cell proliferation and class switch recombination assays, PBMCs were stimulated with 200 ng mL^{-1} CD40 ligand (R&D Systems) and 100 ng mL^{-1} rhIL4 (R&D Systems) for 5 days. For T-cell expansion, PBMCs were stimulated with feeder cells (gamma-irradiated PBMCs) and 1 μg mL^{-1} PHA (Sigma-Aldrich) with 100 U mL^{-1} IL-2 (Peprotech) for 14 days. Expanded T cells were starved by serum deprivation 2 h prior to 200 ng mL^{-1} SDF1 (Peprotech) stimulation. Jurkat E6-1 cells were cultured in complete RPMI-1640 media and stimulated with 2 μg mL^{-1} anti-CD3 (OKT3). Reconstitution with GFP-labeled wild-type *PIK3CG* or empty vector GFP control was performed on a NEPA21 electroporator (Nepagene), according to manufacturer's recommendations, with a poring pulse of 175 V for 5 ms.

Monocyte isolation and differentiation

Primary monocytes were isolated from PBMCs using human Pan Monocyte Isolation Kit (Miltenyi Biotec) according to manufacturer's instructions. To generate human monocyte-derived macrophages, isolated primary monocytes were cultured in complete RPMI-1640 medium (Gibco) with 50 ng mL^{-1} recombinant human M-CSF (Peprotech) for 7 days. Surface markers for human macrophages such as CD163, CD206 were used to stain human monocyte-derived macrophages by flow cytometry. For morphology imaging, human monocyte-derived macrophages were plated on 384-well-plate (PerkinElmer) and stimulated with 250 ng mL^{-1} PMA (Sigma-Aldrich) and 1 μg mL^{-1} ionomycin (Sigma-Aldrich) for 5 h.

Microscopy and image analysis

Following incubation, cells were fixed with 3% Formalin (Pierce) in growth media for 15 min at 37 °C and incubated 15 min at 37 °C in permeabilization buffer (eBioscience) supplemented with 2% heat inactivated FBS (HyClone). Cells were stained first with anti-Tubulin antibodies (1:200, Sigma-Aldrich) for 1 h at RT followed by overnight staining at 4 °C with Phalloidin-Alexa488 (1:500; Thermo Fisher Scientific), DAPI (5 μg/ml, Thermo Fisher Scientific) and AF-555 secondary antibody conjugates (1:1000, Invitrogen). Finally, cells were washed and stored in PBS at 4 °C. Stained cells were imaged using PerkinElmer Opera Phenix high content screening system equipped with 20x (0.4NA) and 40x (1.1NA, water immersion) lenses, confocal unit (Yokogawa CSU-X) and solid state laser illumination (405nm, 488nm, 561nm, 640nm). Each plate was imaged twice: first with 20x lens to image all cells in each well (25x 1080x1080 pxl fields of view (FOV) per well; 640 nm/pxl resolution), followed by imaging with 40x lens to collect high-resolution images of cell footprint (9x 1080x1080 pxl FOV per well; 320 nm/pxl resolution; 3x Z stacks with dZ = 0.5 μm near the coverslip surface). All subsequent measurements were performed using the 20x dataset. 40x datasets were used to create representative images. Quantification of cell area and total amount of F-actin per cell

were done using CellProfiler software and custom written pipeline. Resulting measurements were then further processed using custom written Python scripts. Analysis of significance between donor groups was done using Mann–Whitney *U* test and Bonferroni correction for multiple comparisons.

Flow cytometry

Immunophenotyping was performed on a BD LSR-Fortessa. PBMC staining of surface markers was performed for 30 minutes at 4°C in the dark. The fixation/permeabilization kit for intracellular antigens or transcription factors (Affymetrix, eBioscience) were used for intracellular markers. Frozen PBMCs from patient and healthy donor controls were thawed and allowed to recover for four hours at 37°C in complete media (RPMI-1640 with 10% FBS). Following extracellular staining, cells were stimulated for 15 minutes at 37°C with Dynabeads© Human T activator CD3/CD28 (ThermoFisher) and IL2 (100 IU/mL). Cells were then immediately fixed for 10 minutes at 37°C, washed and permeabilized for 35 minutes on ice. Cells were then stained with p-AKT-PE for 1 hour at room temperature, washed again and resuspended in FACS buffer for flow cytometry analysis. All analyses were performed using FlowJo X (TreeStar Inc.) and Prism 8.0 (GraphPad Software). The following antibodies were used for flow cytometry: From Beckman Coulter: CD16-FITC (clone 3G8), CD4-PECy7 (SFCI12T4D11), CD56-PE (N901), CD56-PECy5 (N901); from eBisocience, Affymetrix: CD4-PerCPCy5.5 (RPA-T4), CD19-PerCPCy5.5 (HIB19), CD69-APC (FN50), FOXP3-APC (236A/E7); from BD Biosciences: CD19-PECy7 (SJ25C1), CD14-PECy5 (61D3), CD16-PECy7 (3G8), CD25-PE (M-A251), CD25-BV605 (2A3), CD27-V450 (M-T271), CD3-APC-H7 (SK7), CD4-BV605 (RPA-T4), CD45RA-AF700 (HI100), CD56-V450 (B159), CD8-V450 (RPA-T8), IgD-FITC (IA6-2), anti-AKT-PE (pS473); from Biolegend: CD163-BV605 (GHI/61), CD206-PE (MMR); from Miltenyi Biotec: IgA-PE (IS11-8E10); IgG-APC (IS11-3B2.2.3).

Immunoblotting

Whole cell lysates were prepared from control- and patient-derived expanded T cells, loaded on 10% acrylamide gel, separated by SDS-PAGE and transferred to a polyvinylidene difluoride membrane (Bio-Rad). Membranes were incubated with 5% BSA in Tris-buffered saline with 0.5% Tween (TBS-T) and were probed overnight with 1:1000 dilution of anti-p110γ (4252) or anti-phospho-AKT Ser473 (D9E) or anti-AKT (pan, 40D4) from Cell Signaling, and 1:8000 dilution of anti-HSP90α/β (Santa Cruz) as a loading control. Bands were revealed using Amersham ECL Select Western Blotting Detection Reagent (GE Healthcare).

Generation of CRISPR/Cas9-edited Jurkat cell lines

sgRNAs targeting *PIK3CG* were designed using the GPP Web portal (https://portals.broadinstitute.org/gpp/public/analysis-tools/sgrna-design) and cloned into a lentiCRISPRv2 using FastDigest Esp3I (Thermo Fisher Scientific) and standard molecular cloning. Lentivirus was generated from transfection of Lenti-X 293T cells (Takara Bio) with Polyfect (Qiagen) using the lentiviral envelope and packing vectors pMD2.g and psPAX2. Lentiviral supernatant was harvested 48 h post transfection, filtered and directly applied to Jurkat E6-1 cells. Transduction was carried out by spinfection (1 h, 37°C, 800 rcf) in the presence of 8 µg mL^{-1} Polybrene. Transduced cells were selected with 1 µg mL^{-1} Puromycin (Sigma). Single clones were selected by limiting dilution and editing was assessed using TIDE.[6] The utilized knockout cells showed 84.6% total editing efficiency, with 21.5% at position +2, 42.9% at position +4 and 19.5% at position -1 after Cas9 cutting site. sgRNA and primer sequences for TIDE were as follows:

For sgRNA,

Fw: caccgAAGTATGACGTCAGTTCCCA,

Rv: aaacTGGGAACTGACGTCATACTTc;

and for TIDE,

Fw: TCTAGCCGTGAAGACCCAGT,

Rv: GCATAATGCTGCTTAATTTTTCAGT.

Phagocytosis assay

The phagocytic function of neutrophils and monocytes was evaluated in 100 µL of sodium-heparinized whole blood sample to 20 µL pHrodo Red *E. coli* (Life Technologies) for 15 minutes at 37ºC according to manufacturer's instructions. Erythrocytes were lysed using reagents provided in pHrodo Red *E. coli* BioParticles Phagocytosis Kit for Flow Cytometry (Life Technologies) and analyzed using flow cytometry (PE channel). Monocytes and neutrophils were distinguished based on forward/side scatter characteristics.

Neutrophil assays

Neutrophils were isolated from whole blood by Ficoll-Paque PLUS (GE Healthcare) density gradient centrifugation. After recovering of PBMCs, the remaining fraction was sequentially pulsed with Milli-Q water and 3 M KCl for erythrocyte lysis, and neutrophils were recovered by centrifugation. Isolated neutrophils were kept in complete RPMI-1640 media, spread on a 10cm culture dish, until further use. For detection of apoptotic cells, neutrophil samples were taken at the indicated time points, replaced by Annexin-V binding buffer (BD Biosciences), and stained on ice for 5 min with propidium iodide (BD Biosciences) and Annexin-V-APC (BD Biosciences), before acquisition by flow cytometry. HD neutrophils treated at 70 °C served as positive control for gate setting. Gating was based on forward/side scatter including live and dead neutrophils. For evaluation of mitochondrial membrane potential, neutrophil fractions were washed in PBS and stained with 3.5 µM JC-1 (Thermo Fisher Scientific) for 15 min at 37 °C. After PBS wash, samples were treated with 100 nM valinomycin in complete RPMI-1640 media. Samples were either taken immediately (0 h) or incubated for 2 h. Cells were gated on single-cell neutrophils by forward/side scatter, and final gates were set on comparing

mitochondrial J-aggregates (PE channel) with cytosolic JC-1 monomers (AlexaFluor488 channel) appearing from mitochondrial membrane leakage. For evaluation of oxidative burst capacities, neutrophils were resuspended in pre-warmed KRP-PBS buffer and placed in a 37 °C thermoshaker. At time point 0, Oxyburst green reagent (Thermo Fisher Scientific, used 1:20) was added and samples were immediately taken at the indicated time points, by pipetting into tubes prepared with ice-cold PBS. For flow cytometry acquisition, an unlabeled sample was taken for peak setting (FITC channel) within the neutrophil scatter gate. For neutrophil chemotaxis, 50,000 neutrophils were placed into the upper chambers of a 96-well transwell plate (Corning, 5 µm pore size), and left to migrate towards 5 nM fMLP or DMSO control in complete RPMI. After 20 min incubation, migrated neutrophils were counted by forward/side scatter detection, and normalized to sample controls of 50,000 neutrophils seeded into the lower compartments, respectively, to reflect total input.

Statistical Analysis

Statistical evaluation of experimental data was performed using Prism version 8 (GraphPad Software, USA). Probability (*P*) values < 0.05 were considered statistically significant. *P* values and statistical tests are indicated in figure legends, where applicable.

SUPPLEMENTARY TABLES

Table S1: Characteristics of the identified germline-encoded *PIK3CG* variants.

Gene	Position	Ref.	Obs.	Substitution	PolyPhen-2	CADD	gnomAD allele counts	ExAC allele counts	ExAC pNull
PIK3CG	Chr7 106545777	A	G	p.N1085S	probably damaging	23.8	---	---	4.4365 E-06
PIK3CG	Chr7 106508151	C	A	p.R49S	benign	22	---	hom: 0, het: 2 (117466), MAF: 1.703 E-05	4.4365 E-06

Prediction scores were calculated with PolyPhen-2 and CADD tools.[4,5] Current genomes include 10,738 (gnomAD, https://gnomad.broadinstitute.org/) and 60,706 individuals (ExAC, http://exac.broadinstitute.org/). MAF frequencies are indicated for identified heterozygotes (accession date: May 21, 2019). Gene names are indicated in italic font. (Ref.: reference; Obs.: observed; het: heterozygous; hom: homozygous; MAF: minor allele frequency; pNull: probability of loss-of-function tolerance; ---: not reported)

Table S2: Extended immunological features of patient T-cell subsets.

Variables	Patient
CD4+ (%)	**61.6** (25-48)
CD45RA+ CCR7+ (%)	45.8 (43.3-63.2)
CD45RA- CCR7+ (%)	40.5 (30.85-45.25)
CD45RA- CCR7- (%)	12.7 (4.2-16.25)
CD45RA+ CCR7- (%)	0.88 (0.1-2.1)
Variables	Patient
CD8+ (%)	12.2 (9-35)
CD45RA+ CCR7+ (%)	60.1 (37-69.35)
CD45RA- CCR7+ (%)	19.7 (14-36.85)
CD45RA- CCR7- (%)	12.2 (2.4-15.5)
CD45RA+ CCR7- (%)	7.98 (3.9-27.25)

Reference ranges are indicated in round brackets. Values out of reference ranges are indicated in **bold** font.

SUPPLEMENTARY REFERENCES

1. Ozen, A. *et al.* CD55 Deficiency, Early-Onset Protein-Losing Enteropathy, and Thrombosis. *New England Journal of Medicine*. 2017;377(1):52–61.
2. Salzer, E. *et al.* RASGRP1 deficiency causes immunodeficiency with impaired cytoskeletal dynamics. *Nature Immunology*. 2016;17(12):1352–1360.
3. Müller, H. *et al.* VCF.Filter: Interactive prioritization of disease-linked genetic variants from sequencing data. *Nucleic Acids Research*. 2017;45(W1):W567–W572.
4. Kircher, M. *et al.* A general framework for estimating the relative pathogenicity of human genetic variants. *Nature Genetics*. 2014;46:310.
5. Adzhubei, I. A. *et al.* A method and server for predicting damaging missense mutations. *Nature Methods*. 2010;7(4):248–9.
6. Brinkman, EK. *et al.* Easy quantitative assessment of genome editing by sequence trace decomposition. *Nucleic Acid Research*. 2014;42(22):e168.

SUPPLEMENTARY FIGURE LEGENDS

Figure S1. (A) Affected amino acid stretches of p110γ are conserved across species. **(B)** Reduced NK-cell frequency in patient peripheral blood. Numerical inserts depict percentages within the final gate. **(C)** Reduced degranulation capacity in patient-derived NK cells, as compared to mother and HD, indicative of impaired cytotoxic capacities. Peripheral blood-derived NK cells were incubated for 3 h with K562 target cells (middle panel) or NK cells activated with IL2 for 48 h prior to K562 target cells (right panel), and compared according to percentages of $CD107a^{+}CD3^{-}CD56^{+}$ cells as a proxy of degranulation ability (* P <0.05, ** P <0.01, Two-way ANOVA). **(D)** Quantification of proliferated $CD8^{+}$ T cells in percentage upon stimulation with various stimuli (** P <0.01, Two-way ANOVA). **(E)** Impaired activation of AKT signaling in *PIK3CG*-mutated patient cells. Patient-derived expanded T cells were stimulated with SDF-1 for the indicated time points. Phospho-AKT signal intensity was compared with total AKT signal. HSP90 was used as housekeeping loading control. **(F)** Abrogated p110γ and reduced p-AKT expressions in *PIK3CG* knockout (KO) Jurkat cells compared to Renilla KO control Jurkat cells. GAPDH was used as a housekeeping loading control. **(G)** Reduced normalized mean fluorescence intensity (MFI) of AKT Ser473 phosphorylation in *PIK3CG* KO Jurkat cells compared to Renilla KO control (** P<0.01, Mann-Whitney U test). Dotted line represents the normalization to unstained control. **(H)** Genetic rescue of $CD69^{+}$ activation (normalized) in *PIK3CG* KO Jurkat cells using wild-type (WT) vector, empty vector (EV), mutant N1085S or mutant R49S vectors (P=0.1, Mann-Whitney U test). **(I)** Intact cytotoxic capacity in patient CTLs compared to cells from mother and HDs. Cells were incubated for 3 h with CD3/CD28 stimulation and compared according to mean fluorescence intensity (MFI) of CD107a (LAMP1) on $CD3^{-}CD8^{+}$ T cell surfaces as a proxy of degranulation ability. **(J)** Increased frequency of peripheral blood $CD4^{+}CD127^{dim}FOXP3^{+}CD25^{+}$ T_{reg} cells in patient, compared to mother and HD. Numerical

inserts depict percentages. **(K)** Patient B cells proliferate normally during 5-day stimulation with CpG or CD40L in combination with IL4 or IL21. **(L)** Class switch recombination capacity of patient B cells is intact after 5-day stimulation with CD40L with IL4.

Figure S2. **(A)** Comparable macrophage surface markers CD163 and CD206 on monocyte-derived macrophages of patient, mother and HD, after 9 days in differentiation culture. **(B)** Violin plots showing average cell number per image of patient, mother and HD. **(C)** Slightly elevated cell death in patient neutrophils. Freshly-isolated neutrophils showed a pronounced propidium iodide-positive population (top, red numerical insert). Apoptotic neutrophils persist during incubation (bottom). Numerical inserts indicate percentages. **(D)** Compromised mitochondrial membrane potential in patient neutrophils. Mitochondria were stained with JC-1 dye, membrane leakage was monitored during incubation with valinomycin. Presence of mitochondrial J-aggregates was compared with appearance of cytosolic JC-1 monomers. Patient neutrophils rapidly lose membrane integrity compared to mother and HD, as observed by the increased dye loss (red numerical insert). Numerical inserts indicate percentages. **(E)** Patient neutrophils are able to initiate oxidative burst upon Fc receptor stimulation as shown by the appearance of oxyburst green-positive cells. **(F)** Patient-derived neutrophils are able to migrate towards fMLP, compared to cells from HDs and mother.

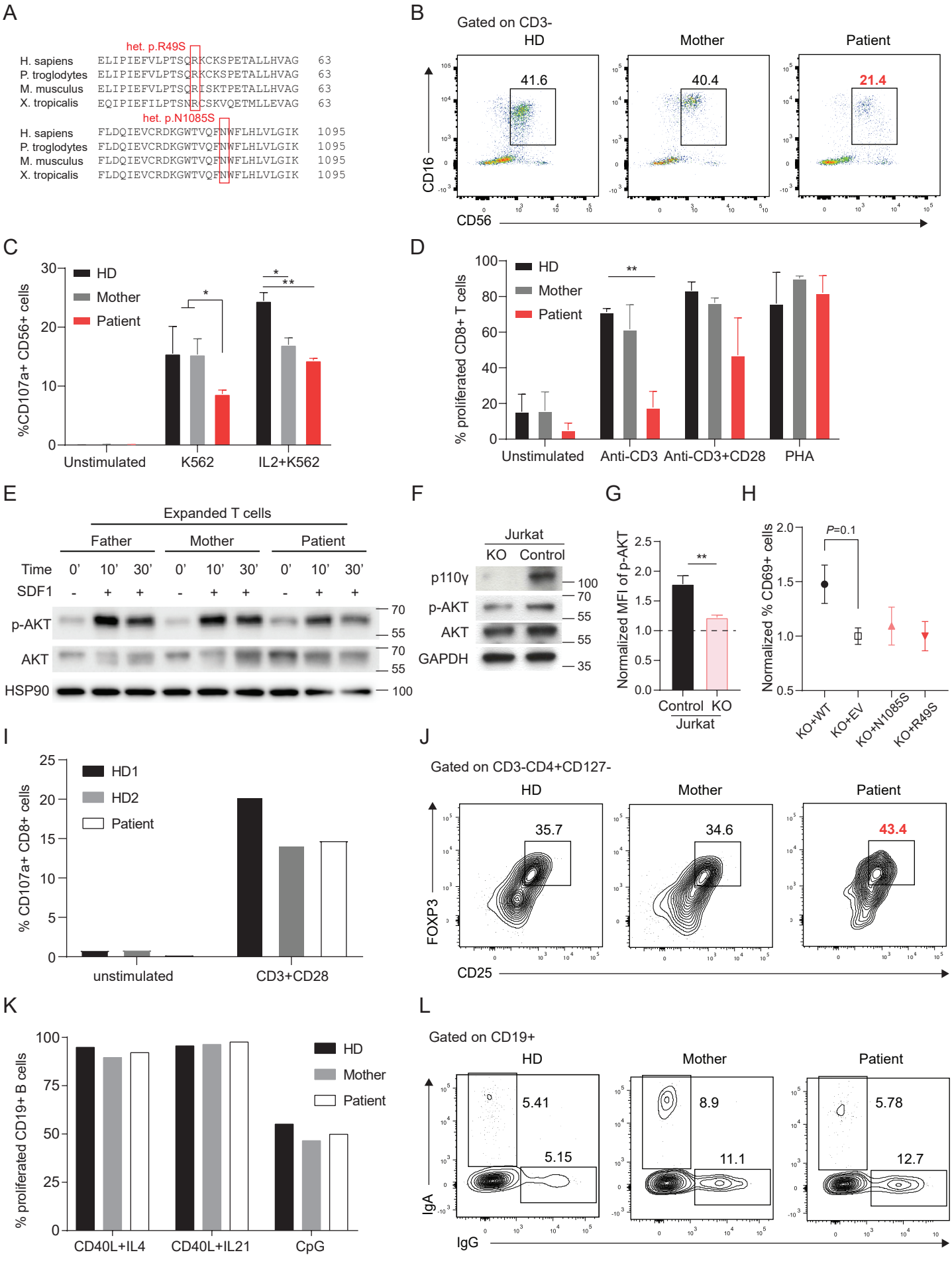

Thian M et al., Figure S1

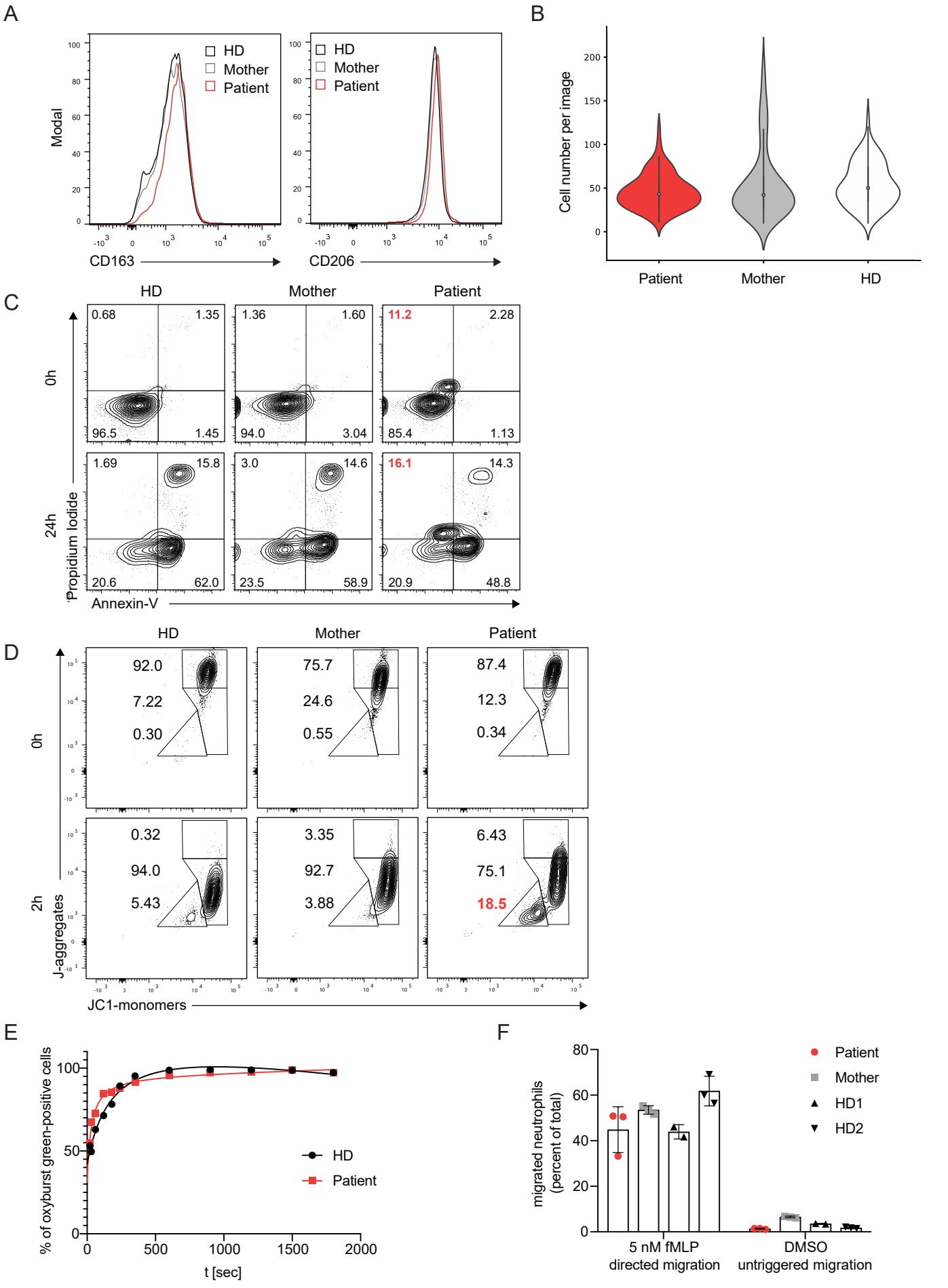

Thian M et al., Figure S2